VELOCITY DEPENDENT FRICTION OF GRANITE OVER A WIDE RANGE OF CONDITIONS

Brian D. Kilgore, Michael L. Blanpied and James H. Dieterich

U. S. Geological Survey, Menlo Park, California

A b s t r a c t. Direct shear sliding experiments on bare ground surfaces of Westerly Granite have been conducted over an exceptionally wide range of sliding rates (10^{-4} μm/s to 10^3 μm/s) at unconfined normal stresses (sn) of 5, 15, 30, 70, and 150 MPa. A new sample configuration was developed that permitted measurements at normal stresses of 70 and 150 MPa without immediate sample failure. Measurements of steady-state velocity dependence of friction at velocities between 10^{-4} and 1 μm/s show similar velocity weakening behavior at all normal stresses, with more negative dependence at lower slip rates. However, at rates above 10 μm/s, velocity weakening is observed only at σ_n = 30, 70 and 150 MPa, while velocity neutral behavior is observed at σ_n = 15 MPa and velocity strengthening is observed at (5, = 5 MPa. The greater velocity weakening observed at velocities below 10^{-2} μm/s may suggest a transition in competing deformation mechanisms, or the influence of additional mechanisms. The transition to velocity strengthening at high velocity and low normal stress implies that rapid slip on shallow faults could be arrested before resulting in true stick-slip behavior. Stable fault creep and creep events observed at shallow levels on some natural faults may result from this transition in velocity dependence.

Introduction

Fault slip occurs by earthquakes, episodic creep or steady creep depending on the manner in which frictional resistance varies with slip rate and displacement. The relationship between sliding friction, slip rate and slip displacement can be described by rate- and state-dependent constitutive relations [*Dieterich*, 1979; *Ruina,* 1983] which have been used to simulate observed laboratory friction behavior and to simulate fault slip in the earth. The constitutive formulation,

$$\mu = \mu_o + A \ln (V / V^*) + B \ln (\theta / \theta^*) \qquad (1)$$

is based on laboratory observations demonstrating that the coefficient of friction, μ, depends on slip rate, V, and the slip history quantified by the state variable θ. The values of the constitutive parameters A, B and the nominal coefficient of friction μ_o are experimentally determined, see Figure 1. The parameters V^* and θ^* are normalizing constants. The value of θ evolves towards a new steady state value; $\theta_{ss} = D_c /V$, after a step change in slip rate to a new slip rate V.

The characteristic distance D_c is the distance required for μ to decay to $\Delta\mu_2 /e$ following a step change in V (see Figure 1). The change in steady state friction, $\Delta\mu_{ss}$, following a step changein V is

$$\Delta\mu_{ss} = (A - B) \ln (V_1 / V_2). \qquad (2)$$

The velocity dependence of steady state friction is parameterized by $A - B$. Steady state velocity weakening ($A - B < 0$) has been shown to be a necessary condition for unstable slip [*Rice and Ruina*, 1983; *Dieterich and Linker*, 1992].

Friction experiments on bare granite at room temperature have shown that $A - B$ varies with slip rate [e.g., *Dieterich* 1978; *Blanpied et al.*, 1997]. Generally, velocity weakening is observed, though A-B can evolve from negative to zero or positive with increasing slip rate [*Blanpied et al.*, 1989]. *Weeks* [1993] notes that a transition to velocity strengthening can limit the peak velocity and total slip during stick-slip instability.

Previous experiments by others have used different experimental designs and limited ranges of slip speeds and/or normal stresses, making detailed comparisons of those data sets somewhat problematic. In this paper, we present new measurements of $A - B$, A and B for initially bare granite surfaces slid at a wide range of unconfined normal stresses (5, 15, 30, 70 and 150 MPa) and slip rates (10^{-4} μm/s ≈ 3 mm/yr to 10^3 μm/s). We use these data to construct plot's of steady state frictional strength vs. slip rate and normal stress. Some
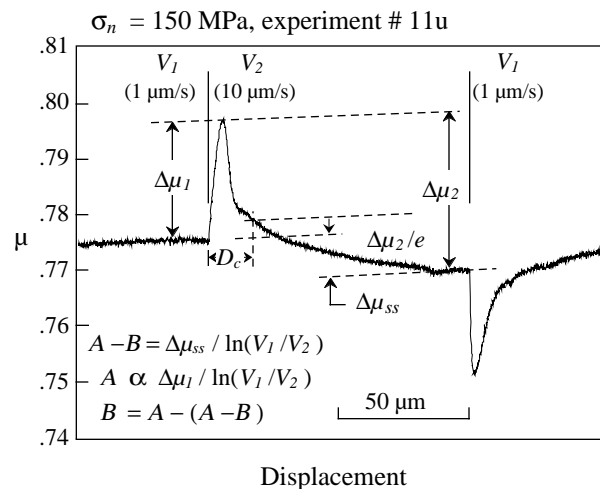

Fig. 1. Transient and steady-state changes of friction, μ for step changes of slip speed, *V*. The initial change in friction in response to a step change in the slip rate is scaled by the parameter *A*. The subsequent evolution of friction to a new steady state level is scaled by the parameter *B*. The velocity dependence of steady-state friction is scaled by *A-B*.

implications of the, results for the behavior of natural faults are discussed.

Experimental Procedure

The sample assembly and apparatus used during these experiments was the three block, sandwich-type direct shear configuration most recently described by *Linker and Dieterich* [1992], Figure 2. Experiment control and the ability to collect high resolution data have been improved by the addition of a new computer system. The computer supplies precise reference signals (16 bit resolution) for the normal stress and slip displacement servocontrol systems, and collects data (12 bit resolution) at rates of up to 50 kHz.

The sliding surfaces of the Westerly granite samples were prepared by hand lapping with #60 SiC abrasive and water on a glass plate. The nominal area of contact between the samples for most of the tests was 50 mm x 50 mm. To achieve unconfined normal stresses of 70 and 150 MPa, a new sample design was developed. Area of contact was reduced on the two smaller, stationary samples by grinding away 90% of the sliding surfaces, leaving a slightly raised square "button" (15.8 mm x 15.8 mm x 1 mm) with tapered sides centered on the sliding surface. The material surrounding the button does not directly support the load, but does provide confinement to the region under the button as stress is applied. This self-confinement strengthens the sample in a manner analogous to the increase of plastic yield strength for indentation compared to uniaxial loading. Two series of tests were performed at σ_n = 30 MPa, one with and one without samples with "buttons", to determine the effect of using this sample configuration.

Velocity dependence was measured after a "run in" of 6 mm while sliding at 10 μm/s [see *Linker and Dieterich*, 1992], Imposed changes of 1 decade in slip velocity were followed by slip at a constant rate, during which sliding friction evolved to a new steady state value. In most cases, slip of 25 μm to 200 μm was needed for μ to reach a nearly steady state value after a velocity step. Values for A -B, A and B were obtained from plots of μ vs. slip displacement. Total displacements ranged from 8.3 mm to 24 mm.

Results

Visual inspections of the samples revealed that a dusting of gouge covered the sliding surfaces after slip at σ_n, = 5 MPa, with more gouge produced at the higher normal stresses. The samples used at (σ_n = 150 MPa produced copious debris and in all cases eventually fractured. Damage up to 10 mm from the sliding surface was revealed by cracks and color variations seen in these broken samples.

Tests comparing samples with and without "buttons" showed that A -B and μ_{ss} agreed within the usual experimental scatter. Tests to monitor displacement-dependent effects μ_{ss} showed that μ_{ss} increased at an average rate of $\approx$ 0.01/mm. This evolution of μ_{ss} was removed from the data by measuring A -B with respect to this trend.

Figure 3 shows representative experiments, and Table 1 summarizes our data. Values for A and B are not reported for V > 10 μm/s due to the inability of the testing apparatus to produce step changes in V at those velocities. Because truly instantaneous changes of slip rate cannot be attained at any V, some rounding of the transient peak occurs, causing measurements of A and B obtained directly from the data to reflect minimum values. Improved determinations of A and B, reported in Table 1, were obtained by applying a correction factor to the measured values. Appropriate correction factors were obtained by simulation of representative experiments using a spring-slider model and a one state-variable constitutive law [see *Tullis and Weeks*, 1986]. Because the testing apparatus is relatively stiff ($\approx$ 1 MPa/μm), we found that using a two state-variable formulation, while improving the overall curve fit between the simulated and recorded data, did not lead to significant improvements in the estimates of A. In the simulations,
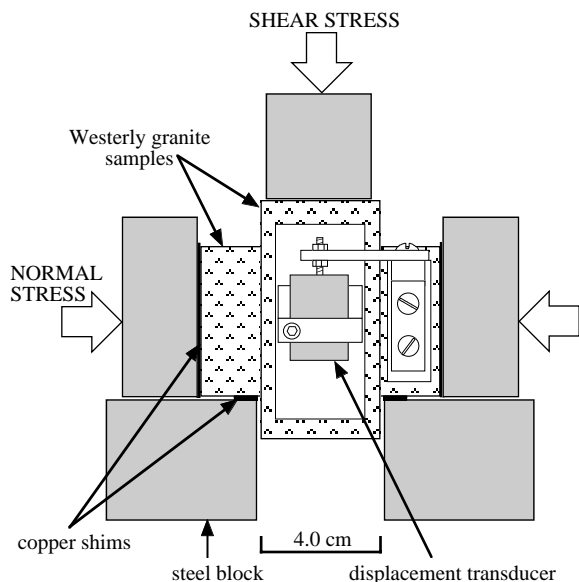

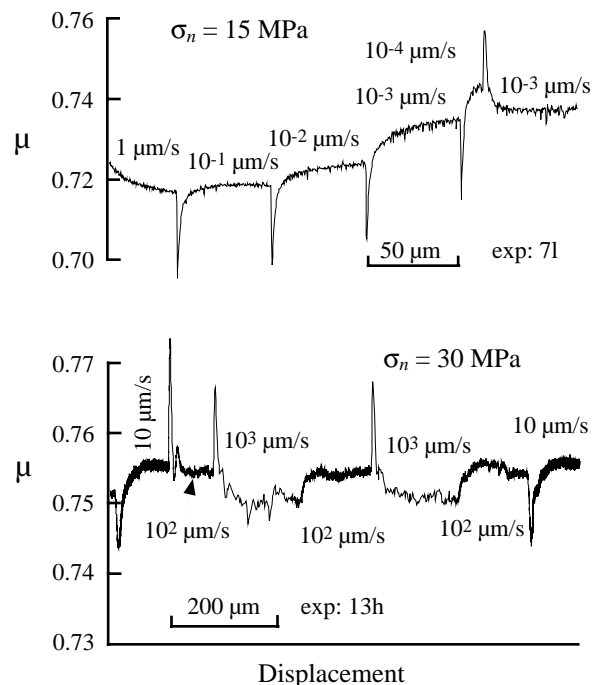Fig. 2. The three block, sandwich-type direct shear sample configuration used in these experiments.

Fig. 3 Representative data from experiments

TABLE 1. Summary of Data

Velocity Interval log(µm/s)	A-B x 10-3	A x 10-3	B x 10-3
σ_n = 5 MPa (3 tests)			
-3 to -2	-3.0 ± 0.5 (2)†	10.3 ± 0.2 (2)	13.3 ± 0.3 (2)
-2 to -1	-1.6 ± 0.5 (14)	11.4 ± 2.7 (15)	13.1 ± 2.8 (14)
-1 to 0	-1.3 ± 0.9 (29)	12.0 ± 3.9 (28)	13.4 ± 3.7 (28)
0 to 1	-0.6 ± 0.9 (28)		
1 to 2	2.0 ± 1.4 (35)		
2 to 3	3.4 ± 1.7 (28)		
σ_n = 15 MPa (3 tests)			
-4 to -3	-3.4 ± 0.3 (2)	10.5 ± 0.6 (2)	13.9 ± 0.9 (2)
-3 to -2	-3.7 ± 1.1 (3)	11.3 ± 1.2 (3)	17.3(1)
-2 to -1	-2.1 ± 0.5 (13)	11.5 ± 2.0 (13)	14.2 ± 3.3 (5)
-1 to 0	-1.6 ± 0.5 (25)	11.5 ± 1.1 (25)	13.4 ± 1.5 (9)
0 to 1	-1.2 ± 1.0 (18)	12.1 ± 1.2 (17)	
1 to 2	-0.1 ± 0.6 (29)		
2 to 3	0.0 ± 1.2 (17)		
σ_n = 30 MPa (2 tests, 1 with regular samples, 1 with button samples)			
-2 to -1	-2.1 ± 0.4 (12)	14.0 ± 2.6 (12)	16.1 ± 2.6 (12)
-1 to 0	-1.4 ± 0.5 (14)	13.5 ± 3.1 (14)	14.9 ± 3.1 (14)
0 to 1	-0.8 ± 0.5 (20)	19.9 ± 5.7 (22)	20.3 ± 8.3 (20)
1 to 2	-1.9 ± 0.8 (27)		
2 to 3	-1.8 ± 0.3 (20)		
σ_n = 70 MPa (2 tests)			
-2 to -1	-1.9 ± 0.5 (4)	13.7 ± 2.2 (4)	15.6 ± 2.3 (4)
-1 to 0	-1.2 ± 0.5 (8)	13.7 ± 1.6 (9)	14.8 ± 2.0 (8)
0 to 1	-1.0 ± 0.4 (23)	12.7 ± 2.0 (26)	13.9 ± 2.0 (23)
1 to 2	-1.6 ± 0.7 (16)		
2 to 3	-2.2 ± 0.4 (14)		
σ_n = 150 MPa (2 tests)			
-3 to -2	-5.0 (1)	12.2 (1)	17.2 (1)
-2 to -1	-0.7 ± 1.1 (13)	11.6 ± 0.9 (13)	12.3 ± 1.1 (13)
-1 to 0	-0.4 ± 0.9 (17)	11.7 ± 0.9 (17)	12.1 ± 1.2 (17)
0 to 1	-0.5 ± 1.0 (69)	13.0 ±10 (106)	12.7 ± 1.2 (68)
1 to 2	-2.7 ± 0.6 (16)		

†Numbers in parenthesis indicate the number of data points

values of D_C were taken as the e-folding distance (see Figure 1) and ranged from 1 to 10 µm, consistent with those reported previously for bare granite surfaces. Generally, values of *A* and *B* reported in Table 1 fall within the range of 11 x 10-3 to 14 x 10-3, independent of normal stress. At σ_n = 30 MPa, *A* and *B* are somewhat greater (13 x 10-3 to 20 x 10-3); the reason for this difference is unclear.

Chester [1988] postulated that frictional heating could influence measurements of *A -B*. He argued that µ has a positive dependence on temperature, and that the temperature of the sliding surface in turn depends on V. Thus, a change in *V* can cause both velocity-dependent and temperature-dependent changes in µ. Chester predicted that at high σ_n and high *V*, "temperature strengthening" could equal or exceed velocity weakening, leading to an apparent velocity neutral or strengthening response. He also predicted that heating of the sliding surface might occur slowly, such that the temperature-dependent response to a change in *V* would be

delayed relative to the velocity-dependent evolution of µ. To test this prediction, we extended the slip displacement between velocity steps to 1 to 2 mm in several runs. In most cases no change in *A -B* was observed. However, at the highest slip rates investigated, steps from 10^2 to 10^3 µm/s, data from (σ_n = 30 and 70 MPa showed a response similar to that predicted by Chester: a short-term velocity weakening response, followed by a delayed rise in µ such that the long-term value of $\Delta\mu_{ss}$, was approximately zero. (Note that *A -B* values cited in Table 1 at these conditions are based on the short term response.)

To better illustrate the effect of *V* on μ_{ss} we plot cumulative changes in μ_{ss} as a function of $\log_{10}V$, Figure 4. Changes in µ, are plotted relative to μ_{ss}, at $\log_{10}V$ = 0. The data correlate well at *V* < 10 µm/s and show increased velocity weakening as *V* decrease. Data collected at *V* > 10 µm/s suggest a relationship between (σ_n and *A -B* . Velocity weakening is observed at $\sigma_n \geq$ 30 MPa. Velocity neutral behavior is observed at (σ_n = 15 MPa, and velocity strengthening is observed at σ_n = 5 MPa.

Discussion

We observe velocity weakening at *V* < 10 µm/s, in agreement with results for bare granite previously reported at various normal stresses between 2 and 100 MPa [e.g., *Dieterich*, 1978; *Tullis and Weeks*, 1986, *Blanpied et al.*, 1987, 1989; *Marone et al.*, 1990]. These observations suggest that unstable stick-slip sliding along faults could occur under a variety of conditions. The enhanced velocity weakening observed at *V* < 10-1 µm/s may reflect a change in the relative importance of competing deformation mechanisms or the influence of additional deformation mechanisms such as crystal plasticity or subcritical crack growth.

A new observation is that at slip rates above 10 µm/s, the sign of *A -B* depends on normal stress. The switch to velocity strengthening at low a, and high *V* is interesting; however the basis for this switch is not clear. Velocity strengthening has been previously reported for granite [e.g., *Lockner et al.*, 1986; *Marone et al.*, 1990; *Stesky*, 1978] and has frequently been attributed to the presence of a layer of
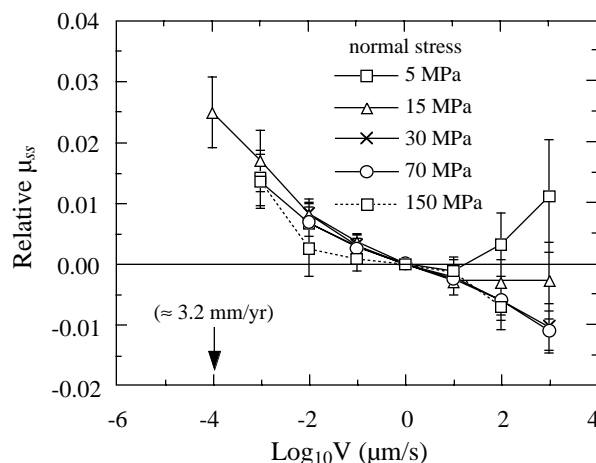

Fig. 4. Relative steady-state friction vs. $\log_{10}V$. Error bars represent the cumulative one standard deviation error measured from data at $\log_{10}V$ =0.

simulated gouge or elevated temperatures. *Marone* et al. [1990] observed velocity weakening in tests on bare granite, but velocity strengthening in tests with simulated gouge. The magnitude of the velocity strengthening they observed in tests with gouge varied inversely with a, and directly with the thickness of the gouge layer. They concluded that the observed velocity strengthening was due to rate-dependent dilatancy of the gouge. However, measurement of the horizontal dimensions of the three-block sample during our tests at σ_n = 5 MPa showed no dilatancy as slip rates reached 10^3 μm/s. This is not surprising, since little gouge was produced in our tests at σ_n = 5 MPa.

Chester [1988] and *Blanpied et al.* [1989] suggested that frictional heating can cause a transition to velocity strengthening. Blanpied et al. [1989 and unpublished data] measured velocity dependence and frictional heating for bare granite surfaces and inferred that there exists a critical heating rate, Q = shear stress (τ) x V, above which granite shows velocity strengthening. They estimated Q to be ≈ 2.0×10^{-4} MPa·μm/s, Our observations of velocity strengthening at σ_n = 5 MPa, τ ≈ 3.5 MPa and V = 10^3 μm/s (Q ≈ 0.4×10^4 MPa·μm/s) run counter to this explanation. The highest heating rates encountered during our experiments were at (σ_n = 30 MPa (τ ≈ 21 MPa) and 70 MPa (τ ≈ 49 MPa) and V = 10^3 μm/S (Q = 2.1×10^4 and 4.9×10^4 MPa μm/s) where transitions from velocity weakening to velocity neutral rate-dependence were observed after sufficient displacement. As suggested earlier, the delayed rise in friction observed at these conditions may be due to frictional heating.

Conclusions

The observed relationships between velocity-dependent friction on bare granite surfaces and normal stress have significant implications for the dynamics of natural fault systems. The laboratory observations of velocity weakening behavior on bare granite surfaces under a wide variety of conditions suggests that stick slip sliding could be the prevalent form of slip along some faults. The increase in velocity weakening at the lowest slip rates may suggest the transition in or the influence of other deformation processes. The transition to velocity strengthening at low normal stresses and high slip rates implies that accelerating slip on shallow faults could be arrested before reaching seismic slip rates. This is consistent with creep events observed at shallow depths on some natural faults.

References

Blanpied, M.L., T.E. Tullis and J.D. Weeks, Frictional behavior of granite at low and high sliding velocities, *Geophys. Res. Lettr., 14*, 554-557, 1987.

Blanpied, M,L., J.D. Weeks and T.E. Tullis, Effects of sliding rate and shear heating on the velocity dependence of granite friction, *EOS, Trans. AGU, 70*, 1303, 1989,

Chester, F. M., Temperature and rate dependence of friction for faults, *EOS, Trans. AGU, 69*, 471, 1988.

Dieterich, J.H., Time-dependent friction and the mechanics of stick-slip, *Pure Appl. Geophys., 116*, 790-806, 1978.

Dieterich, J.H_ Modeling of rock friction 1. Experimental results and constitutive equations, *J, Geophys, Res., 84*, 2161-2168, 1979.

Dieterich, J.H. and M.F. Linker, Fault stability under conditions of variable normal stress, *Geophys. Res. Lettr., 19*, 1691-1694, 1992,

Linker, M.F. and J.H, Dieterich, Effects of variable normal stress on rock friction: Observations and constitutive equations, *J. Geophys, Res., 97*, 4923-4940, 1992.

Lockner, D.A., R. Summers and J.D. Byerlee, Effects of temperature and sliding rate on frictional strength of granite, *Pure Appl. Geophys., 124*, 445-469, 1986.

Marone, C., C.B. Raleigh and C.H. Scholz, Frictional behavior and constitutive modeling of simulated fault gouge, *J. Geophys. Res., 95*, 7007-7025, 1990.

Rice, J.R. and A.L. Ruina, Stability of steady state frictional slipping, *J. Appl. Mech., 50*, 343-349, 1983.

Ruina, A.L., Slip instability and state variable friction laws, *J. Geophys. Res., 88*, 10359-10370, 1983.

Stesky, R.M., Mechanisms of high-temperature frictional sliding in Westerly granite, *Can. J. Earth Sci., 15*, 361-375, 1978.

Tullis, T.E. and J.D. Weeks, Constitutive behavior and stability of frictional sliding of granite, *Pure Appl. Geophys., 124*, 384-414, 1986.

Weeks, J.D., Constitutive laws for high velocity frictional sliding and their influence on stress drop during unstable slip, *J. Geophys. Res.*, in press, 1993.

_____

M. Blanpied, J. Dieterich and B. Kilgore, U. S. Geological Survey, MS-977, 345 Middlefield Rd., Menlo Park, CA 94025.